Kinetico-mechanistic studies of substitution reactions on cross-bridged cyclen CoIII complexes with nucleosides and nucleotides†

Marta Vázquez,[a] Mercè Font-Bardia[b] and Manuel Martínez*[a]

aDepartament de Química Inorgànica, Universitat de Barcelona, Martí i Franquès 1-11, E-08028 Barcelona, Spain.
E-mail: manel.martinez@qi.ub.es

bUnitat de Difracció de RX, Centres Científics i Tecnològics de la Universitat de Barcelona (CCiTUB), Universitat de Barcelona, Solé i Sabarís 1-3, 08028-Barcelona, Spain

Kinetico-mechanistic studies on the substitution reactivity of the [Co{(μ-ET)cyclen}(H2O)2]3+ complex cation at pH values within the 6.0–7.0 range with biologically significant ligands have been carried out. The substitution processes have been found to occur exclusively on the mono-hydroxobridged [(Co{(μ-ET)cyclen}(H2O))2(μ-OH)]5+ species formed after equilibration of the cobalt complex in the relevant medium. The studies conducted on the substitution of the aqua/hydroxo ligands of this dinuclear species are indicative of a dominant role of outer-sphere complexation, involving hydrogen-bonding interactions. The values of the outer-sphere complex formation equilibrium constant are in line with the intervention of both the exiting aqua ligands and the NH groups at the encapsulating {(μ-ET)cyclen} ligand. These complexes result in the preferential formation of O- or N-bonded nucleotides depending on the structure of the base moiety of the ligand. Even the entry of the different donor bonded nucleotides is hampered by the hydrogen-bonding interaction with the dangling moiety of an already coordinated ligand. In general the overall substitution processes occur at a faster rate than those published for the fully alkylated encapsulating {(Me)2(μ-ET)cyclen} ligand derivative, as expected for the still available base-catalysing NH groups in the {(μ-ET)cyclen} ligand.

INTRODUCTION

As stated on many occasions, the use of coordination compounds to study possible modification in biologically significant molecules is not new, nevertheless any new information that can be extracted from their simple reactivity should not be underestimated.1,2 Besides obvious thermodynamic requirements and no leaching of the metal centre, the need for the processes to occur at a rate that allows a controlled reaction, should also be taken into consideration when designing systems able to act in biological systems. That is, the solvolysis or substitution processes that involve the metal centres have to be relatively slow in order to ascertain the maintenance of the active molecule, or the interaction of the complex with the expected target.3 Nevertheless, the use of complexes that behave as dead-end species for kinetic or thermodynamic reasons should also be avoided. A significant amount of literature has been lately appearing dealing with the speciation, hydrolysis, complexation and polymerization of a number of "biologically" active centres, underlining the key role of simple substitution processes actuating on biologically relevant coordination complexes.4–7 Clearly a rationalization of the solution behaviour of metal complexes under conditions similar to those in biological media is fully desirable, including stability in plasma studies.8 Mimicking in vitro the conditions of biological systems is extremely difficult, if possible at all, so that some simplifications have to be made. In this respect, hydrogen bonding and stabilization of supramolecular interactions have dramatic consequences in many processes expected to be rather simple.9 Another important aspect relates to the effect of temperature on the activity of these coordination compounds,10 which underlines the importance of determining activation parameters for these simple substitution reactivities, a point normally not considered.

Although the anticancer activity of cis-platinum still remains as the most important landmark in medicinal inorganic chemistry, the importance of other metal complexes should not be underestimated.11 The last few decades have seen an increasing number of reports showing metal complexes with promising medical applications and, for example, ruthenium complexes are now one of the most important groups of compounds with antitumor properties.12–17 CoIII complexes with an inert tetradentate skeleton and two reactive positions in cis are obviously interesting as they could represent a cheaper and less toxic alternative to currently used compounds.18 Even some Co alkyne complexes have shown promising activity associated with their capability to target specific enzymes.19,20 The use of complexes of type cis-[Co(N)4(H2O)2]3+, with (N)4 being tren, cyclen or fully alkylated {(Me)2(μ-ET)cyclen} has already been explored by us9,21,22 by studying their substitution processes with some nucleosides and nucleotides at physiological pH. In this respect there has been an important increase in the use of cross-bridged cyclen and cyclam ligands, both for their promising properties and the robustness of their structure containing five- and six-membered macrocyclic full encapsulation.23–25 Although for the tren and cyclen complexes the existence of fast base-conjugate processes dominate their reactivity,26–29 the use of the fully substituted [Co{(Me)2(μ-ET)cyclen}(H2O)2]3+ produces a definite increase in the inertness of the derivatives, due to the absence of acidic NH groups.27 In this respect, the formation and cleavage of hydroxo-bridged dimeric units, kineticomechanistically detected some time ago,30,31 has been found to be a keystone. The prevalence of reasonably reactive dinuclear mono-hydroxo-bridged species is directly related to the presence of these NH groups, only dead-end {(N)4Co(μ-OH)2Co(N)4} cores detected at pH > 7.2 for the fully alkylated [Co{(Me)2(μ-ET)cyclen}(H2O)2]3+ material.

In view of these facts, the study of the complex with the tuned, partially substituted but conformation-rigid, {(μ-ET)-cyclen} (Scheme 1, top) cyclen-based ligand has been pursued. By the use of this ligand, base-conjugate accelerated substitution processes would still be active at pH values normally higher than neutrality, once the extremely acidic equatorial NH groups in cyclen have been substituted.29 Furthermore, the presence of acidic hydrogens attached to the axial nitrogen donors should also allow some of the interactions observed for the [Co(cyclen)(H2O)2]3+ complex9 with Good's buffer media,32 as well as in ZnII complexes with nucleotides.33 In this report we present the study of the spontaneous

solution chemistry of [Co{(μ-ET)cyclen}(H2O)2]3+ in a pH range close to neutrality, as well as the kinetico-mechanistic studies on its substitution reactivity with chloride, inorganic phosphate and the nucleosides and nucleotides indicated in Scheme 1. The results collected agree with the reactivity of the CoIII t2g 6 metal centre in dinuclear [{Co{(μ-ET)cyclen}-(H2O)}2(μ-OH)]5+ units. The processes are also slightly accelerated, with respect to those observed for the fully substituted {(Me)2(μ-ET)cyclen} analogue, by the actuation of a base-conjugate pathway. Reactivity stops at pH > 7.5, where the prevalence of the bis-hydroxo dimeric form of the ion occurs. The data collected are also indicative of important outer-sphere interactions between the donors on the nucleobase moieties and both the remaining NH axial groups of the encapsulating ligand, and the aqua ligands on the CoIII coordination centre.

RESULTS AND DISCUSSION

Solution behaviour of [Co{(μ-ET)cyclen}(H2O)2]3+ in the 5.5–7.5 pH range

The diaquo [Co{(μ-ET)cyclen}(H2O)2]3+ complex has been obtained for the first time in this work as a triflate salt, and XRD analyses of the compound has also been carried out (Fig. 1). Distances and angles determined for the cation complex do not show any significant difference with those from the cyclen34 and {(Me)2(μ-ET)cyclen}18 related complexes. The values of the two pKas for this species have been determined, both by potentiometric and spectrophotometric NaOH titrations at I = 1.0 (NaClO4), as 5.1 and 7.4 at 25 °C, as indicated in the Experimental section. With these values in hand, the species present in the pH margin of our kinetic studies are [Co{(μ-ET)cyclen}(H2O)(OH)]2+ and [Co{(μ-ET)cyclen}(OH)2]+. Determination of these pKa values using different pH equilibration times (i.e. 10–70 seconds) was also carried out with the same outcome, thus indicating that the processes being measured correspond effectively to the deprotonation equilibria with no significant intervention of secondary processes. Once the acid/base prevalent species at physiological pH was established, the possible polymerization processes occurring due to the generation of bridging hydroxo ligands on increasing the pH was pursued.9,22,28,35 Studies conducted on (5–10) × 10−4 M solutions of the [Co{(μ-ET)cyclen}(H2O)2]3+ complex, in non-buffered final pH = 7.5, show a set of two step changes in the UV-Vis spectrum on the 30 minute time-scale. By comparison with the previous solution chemistry of the parent [Co(cyclen)(H2O)2]3+ and the fully alkylated [Co{(Me)2(μ-ET)-cyclen}(H2O)2]3+ complexes,9,22 the reactions have been associated with the sequential formation of mono- and bis-hydroxobridged, [(Co{(μ-ET)cyclen})2(μ-OH)2]4+, complexes.

By the use of MES and HEPES buffers, a pH screening of this spontaneous solution reactivity has been conducted. In all cases the mentioned UV-Vis spectral changes are reproducible (Fig. S1†), and show the two-step sequence indicated above. The time-scale of these processes (10 plus 70 minutes at 17 °C) is clearly intermediate between those observed for the parent cyclen9 and those found for the fully substituted {(Me)2(μ-ET)-cyclen}22 analogous derivatives. This trend is in line with the residual presence of two slightly acidic NH axial groups attached to the CoIII centre in the present compound, still capable of induced base-catalysed substitution reactivity.29,36 At the same time-scale, for the parent cyclen derivative, the presence of very acidic equatorial NH groups,29 induce fast polymerization reactions.9 As found for the previously studied related systems, the absorbance changes increase significantly with increasing pH, but can be reversed in a fast process by addition of HClO4 to acidic pH. At pH > 7.5 the changes associated with the second process become very important and are related to the lack of reactivity observed with the variety of ligands studied (see the following section).

Summarising, the behaviour of the [Co{(μ-ET)cyclen}-(H2O)2]3+ system has intermediate features between those of the parent cyclen9 and {(Me)2(μ-ET)cyclen}22 derivatives. The polymerisation equilibria indicated in Scheme 2 are at pH values higher than 7.5 (after 30 minutes at room temperature, see below) significantly displaced to the formation of a dimeric dead-end bis-hydroxo [(Co{(μ-ET)cyclen})2(μ-OH)2]4+ complex. At lower pH values (within the 6.0–7.0 range) the mono-hydroxobridged dinuclear species is prevalent on equilibration for a few minutes, and reactivity is, consequently, expected from the aqua ligands.9,22

Substitution reactions on [Co{(μ-ET)cyclen}(H2O)2]3+ in the 6.0–7.5 pH range by chloride, phosphate, cytidine, thymidine, uridine, 5′-cytidinemonophosphate, 5′-thymidinemonophosphate and 5′-uridinemonophosphate

After the knowledge of the solution nature of the equilibrated species of the [Co{(μ-ET)cyclen}(H2O)2]3+ complex in the 6.0–7.5 pH range, and in view of some studies carried out on this

core in biologically relevant processes,18,37 the reactivity at physiological pH of the complex was pursued. For the parent cyclen and {(Me)2(μ-ET)cyclen} complexes at these pHs,9,22 no reactivity with chloride had been observed, which is relevant in view of the chemistry of cis-platinum at different pCl.38–41 For the present complex, the substitution of the aqua/hydroxo ligands at pH values between 6.0 and 7.5 and at [Cl−] = 0.05–0.075 M is also not observed after 24 hours at 40 °C.

Phosphate. As a follow up, the reactivity of the complex with simple inorganic phosphates was studied as a model for the substitution processes occurring with nucleotides. Furthermore, the process has a perfect spectroscopic NMR handle21,42 for the establishment of the nature of the reacting and final complexes. Monitoring the spectral changes on non-equilibrated, freshly prepared, solutions of compound [Co{(μ-ET)-cyclen}(H2O)2]3+, with phosphate leads to a complex sequence where the fastest changes were equivalent to those observed for solutions not-containing the ligand. Thus, by using the methodology indicated in the Experimental section,9,21,22 the time-resolved UV-Vis spectral changes occurring on pre-equilibrated (30 minutes at room temperature) samples of [Co{(μ-ET)-cyclen}(H2O)2]3+ at the relevant pHs were monitored instead. The changes observed (Fig. 2a) in the UV-Vis spectrum, can be fitted to a two-step reaction sequence with rather similar rate constants that were obtained as described in the Experimental section.43,44 While a definite limiting dependence, i.e. kobs1 = KOS × k1[phosphate]/(1 + KOS[phosphate]), on the total concentration of phosphate is evident for one of the steps observed, no dependence on concentration is obtained for the other step in the sequence (Fig. 2b). Clearly the limiting first-order rate constant obtained from these plots corresponds to the coordination of a phosphate anion on a precursor outersphere encounter complex (as already been established for other phosphorous oxoanion substitution reactions).45–47 Consequently, the other reaction should correspond to a consecutive chelation, or bridging, of the ligand after its coordination. Table 1 shows the relevant kinetic data for these processes.

For the concentration dependent (k1) path, the limiting behaviour agrees with that observed for the parent cyclen complex, but is contrary to that for the {(Me)2(μ-ET)cyclen} analogue.9,22 Clearly, as found in other systems,33 the available and well-oriented NH groups in the macrocyclic ligand promote such outer-sphere association complexes with the entering anion (avKOS = 120 M−1 in this case). As for the outcome of the concentration independent (k2) path, 31P NMR spectroscopy of the final reaction mixtures indicated the presence of a phosphato ligand with either a η2 or μ geometrical arrangement (20 ppm downfield from the signal of the free anion).42 Experiments carried out with a [Co] : [P]total = 1:5 ratio produced a final [P]total : [P]20 ppm = 4.5 : 0.5, thus indicating that a simple [(Co{(μ-ET)cyclen})2(μ-OOPO2)(μ-OH)]2+ complex is formed after the reaction (Scheme 3, top). The same arrangement has been observed for the parent unsubstituted cyclen derivative,9 which is in line with that indicated in Scheme 2. Finally it is interesting to note, as seen both in Fig. 2b and Table 1, that, although some pH trends might be present in the rate constants determined, these are not significant; the reactions seem to be pH independent in the narrow range studied (6.0–7.0). In view of the reactivity observed, completely parallel to that for the parent cyclen derivative,9 the thermal and pressure activation parameters for this system have not been determined.

Cytidine. The study of substitution reactions on the above mentioned CoIII complex with biologically relevant ligands with nitrogen donors, i.e. nucleosides or nucleobases, was further intended (after the equilibration indicated in the previous section). No changes were observed at pH ≥ 7.5, in good agreement with the formation of the dead-end bis-hydroxobridged dimers (Scheme 2), and the reaction was only studied in the 6.0–7.0 pH range, where the [(Co{(μ-ET)cyclen}(H2O))2(μ- OH)]5+ species is prevalent in the medium. By using the standard software,43,44 these changes were associated with a twostep sequential process. Water Presat proton NMR experiments on the reacting solutions established the nature of the two species appearing during the process. The spectrum collected after 1 hour of reaction at 40 °C at pH = 6.1 shows, apart from the intense doublet at 7.8 ppm corresponding to the para-NH proton of the ring of the free cytidine, a signal at 7.7 ppm. After further 24 hours under the same reaction conditions, the signal at 7.7 ppm increases its intensity and a new signal appears at 7.6

ppm. These data agree with the initial formation of a mono-cytidine complex (7.7 ppm) that evolves to a bis-cytidine species (7.6 ppm) with time (Fig. S2†) in an equilibrium overall process. Fig. S3† shows the trends observed for the two pseudo-first order rate constants with the concentration of cytidine; the values derived at different pHs are shown in Table 1. From these plots it is clear that an equilibrium condition is established for both substitution reactions (as indicated by the NMR data). The equilibrium constants (10–40 M−1 for K1 and 50–90 M−1 for K2) indicate a definite preference for the bissubstituted [(Co{(μ-ET)cyclen}(cytidine))2(μ-OH)]5+ complex. The slight acceleration (see Table 1) of the rate on increasing the basicity of the medium is in good agreement with the residual operation of a conjugate-base mechanism due to the existence of NH groups in the cobalt encapsulating ligand used. Given the complexity of the data only the thermal activation parameters at pH = 6.5 have been determined. For ΔH‡, the values indicate in all cases a high degree of dissociativeness, as expected for CoIII complexes when conjugate-base mechanisms might be operative. The values for the activation entropies are also positive, but less than expected for this type of activation, especially as k1 and k2 on rate constants are concerned. The inclusion of the outer-sphere association constants in the value used for the determination of these parameters might be responsible for the lesser degree of dissociativeness observed.

Thymidine. Initially, as for previous studies,22 thymidine (Scheme 1) was chosen due to the neutral characteristics of its nitrogen donor (pKa = 9.8),48,49 which allows for a simplification of the system, despite its anionic nature once coordinated to the CoIII centre.33 Fig. 3a shows the typical UV-Vis spectral changes observed in the system and Fig. 3b shows the trends for the pseudo-first-order rate constants obtained at different acidities for this substitution process with thymidine. While the slow step (kobs2) shows a linear dependence on the concentration of the entering ligand, the fastest step (kobs1) clearly shows a limiting behaviour22,35,50,51 on the thymidine concentration (as already found for the phosphate substitution process, see above). As in previous studies, no dependence on the pH is observed, and the limiting value of the fast step (k1 (s−1)) and the slope of the dependence of the second step (k2 (M−1 s−1)) were obtained from an average of the data at the same thymidine concentrations at different pHs. The relevant data extracted from these plots indicated are shown in Table 1.

Thus, as for cytidine, the substitution reaction of complex [Co{(μ-ET)cyclen}(H2O)2]3+ with thymidine at pH values between 6.0 and 7.0 corresponds to a process occurring on the mono-hydroxo bridged [(Co{(μ-ET)cyclen}(H2O))2(μ-OH)]5+ species prevalent in this medium (see Scheme 3, bottom). The reaction produces the bis-substituted [(Co{(μ-ET)cyclen}(thymidine))2(μ-OH)]3+ species as the final complex via a clear dissociative activation mechanism for each sequential step. This is evidenced by the large values of ΔH‡ (Table 1) of the same magnitude than those found for similar dissociatively activated CoIII amine complexes.52–54 Interestingly, the values determined for ΔS‡ are practically zero, and the volumes of activation are negative for the k1 process and positive for the k2 step. This unexpected trend in the values of ΔS‡, and their lack of correlation with ΔV‡, has been related to the existence of important solvent assisted hydrogen bonding interactions in the transition state of the substitution process.55–59 This is not surprising in this case, the nature of both the entering and encapsulating ligands (see Scheme 1) should be prone to hydrogen bonding interactions. In this respect, the previously reported22 reaction of [Co{(Me)2(μ-ET)cyclen}(H2O)2]3+ with 5′-TMP is a clear example of this effect in this family of substitution processes.

In contraposition with that observed for the cytidine substitution, where no acidic protons are available in the ligand, for the entry of the first thymidine nucleoside the reaction involves the limiting formation of an outer-sphere encounter precursor complex (KOS = 240 M−1, Fig. 3b and Table 1), as found for other substitution reactions on CoIII amine systems,47,60 as well as on the related [Co{(Me)2(μ-T)cyclen}-(OH)(H2O)]2+ complex.22 The formation of this outer-sphere complex has been associated with the interaction of the proanionic {ONO} unit of the nucleoside (see Scheme 1) both with the protons of the remaining aqua ligand in the CoIII complex at this pH and the NH groups in the ligand.33 Effectively, for this nucleoside the value of KOS is an order of magnitude larger than for the not-

containing NH group analogue systems studied.22 As for the entry of the second thymidine ligand, the value of the outer-sphere association equilibrium constant has definitively decreased in a way that a simple linear dependence between the value of kobs2 and [thymidine] is obtained (Fig. 3b). The decrease of the positive charge of the CoIII complex, produced by the first substitution of H2O by thymidine (which involves its deprotonation to the thymidine{–H} −anionic ligand)7,33 can easily explain this fact.

The fact that the water by thymidine substitution reactions are not affected by the pH in the narrow range studied is somehow surprising. A compensation effect between the increasing amounts of the more labile H2O/OH− CoIII species on decreasing the pH, and the viability of an accelerated baseconjugated substitution on its increase, seems to result in the final outcome observed. Furthermore, the protonation ambiguity effect on putative full hydroxo outer-sphere complexes can also explain this fact for the first nucleobase entry.61

Uridine. The substitution process with a very similar uridine nucleoside (Scheme 1) was also pursued and a completely parallel behaviour with respect to the substitution by thymidine (Fig. S4†) has been observed. The slightly higher values of the rate constants can be associated with its lower steric requirements (see Scheme 3). Furthermore, its higher (pKa = 9.3)62 acidity also weakens the outer-sphere association of the {ONO} unit of the nucleoside, as observed from the less pronounced curvature for the k1 versus [uridine] trend (Fig. S4a†). Given the similarity obtained with the thymidine studies above, as well as the expected character of the variations observed, no further studies related to pH variation and activation parameters were conducted.

5′-CMP. Once the reactivity with phosphates and nucleosides was established, the substitution processes by nucleotides was pursued;9,22 the 5′-CMP nucleotide has been our first choice due to the similar anionic behaviour to phosphate anions, as well as for its non-pro-anionic nature on the nucleoside moiety. Effectively, as for the H2PO4−/HPO42− system the spectral changes indicate a two-step reactivity pattern at 40 °C within the 6.0–7.0 pH range, where the ligand is in the 5′-CMP−/5′-CMP2− forms.63 The global fitting of these timeresolved changes43,44 produced a series of rate constants that are concentration dependent for the two consecutive steps (Fig. S5†). 31P NMR spectroscopy indicated that an initial species is formed showing a signal at 9.4 ppm downfield from that of the free ligand, followed by the appearance of another signal at 14.1 ppm also downfield from that of the free ligand. Both signals coexist in the final reaction mixture and correspond to mono-dentate phosphato ligands involved in equilibrium (Fig. S6†). The full reaction scheme for this system, parallels what has been observed for the parent [Co(cyclen)-(H2O)2]3+ compound (Scheme 4, top).9 The fact that no induction period has been observed in the NMR experiments, and that the shift in the UV-Vis occurs to lower energies, is also an indicative of the neat formation of O-bound 5′-CMP complex. The data collected in Table 1 indicate that, in contrast to the observed for the reaction with inorganic phosphate, the reaction rate increases with pH. The increasing presence of fully deprotonated 5′-CMP2− (pKa = 6.1) species, not so much relevant for inorganic phosphate (pKa = 7.21), seems to be decisive.42,63

The absence of a measurable value of KOS for the substitution by 5′-CMP, when compared to that with inorganic phosphates, is in line with an intermediate behaviour from that observed for the reactions with [Co(cyclen)(H2O)2]3+ and those with [Co{(Me)2(μ-ET)cyclen}(H2O)2]3+.9,22 Clearly the presence of NH groups in the ligand structure (see Scheme 1) plays a determinant role in the outer-sphere association with the smaller H2PO4−/HPO42−, which is not possible with the more encumbered 5′-CMP−/5′-CMP2− anion. Nevertheless, additional hydrogen bonding interactions with the solvent may also be a competing factor to account for the weaker interactions observed between the CoIII complex and the ligand in this case. From the data in Table 1 the values of K1 and K2 are found equivalent considering the methodological errors involved, their values are apparently also independent of the pH and within the 7–11 M−1 range.

As for the thermal activation parameters shown in Table 1 for this system, it is interesting to note that, while for the first entry of 5′-CMP the direct process has all the characteristics of a dissociatively activated reaction, for the entry of the second ligand a much higher degree of associativeness is observed. The same is observed for the aquation reaction occurring on the same material, i.e. [(Co{(μ-ET)cyclen}(5′-CMP))(μ-OH)-(Co{(μ-ET)cyclen}(H2O))]3+ (Scheme 4). It is clear that, although a dissociatively activated substitution mechanism is expected for tetraamine CoIII complexes, especially when a conjugatebase process can be operative,28,36 outer-sphere interactions lead to a certain degree of association which also facilitates the reaction. It is clear that the nature of the complex plays a key role in the above mentioned interactions, especially taking into account the presence of two NH groups in the macrocyclic ligand of the inert skeleton. In fact a recent report has appeared in reference to such outer-sphere interactions as responsible for deeply tuning the electronics of rather simple complexes.64

5′-TMP. The substitution reactions with the 5′-TMP nucleotide (Scheme 1) were studied to generalise the interesting substitution trends observed for the different phosphates with this CoIII complex.22 The nature of this nucleotide allows the formation of anionic N- and O-bound nucleotide complexes. As for the previous systems in the present report, the timeresolved UV-Vis spectral changes can be fitted to a two-step sequence with the concentration and pH dependence characteristics indicated in Fig. 4. 31P NMR experiments were conducted to establish the nature of the product of the two set of consecutive processes. After 30 minutes at 40 °C and pH = 6.5 the only signal appearing in the 31P NMR corresponds to that of the free ligand (2.9 ppm), while after a further period of 10 hours a new signal at 12.6 ppm appears, corresponding to a mono-dentate O-phosphate. The relative intensity of these 31P NMR signals indicate the entry of a single phosphate ligand per each CoIII 2 unit, thus indicating the validity of the implied reactive species indicated in Schemes 2 and 4 in this narrow pH range. It is thus clear that the same behaviour observed for the fully alkylated derivative is operative:22 formation of [(Co{(μ-ET)cyclen}(N-5′-TMP))(μ-OH)(Co{(μ-ET)-cyclen}(H2O))]4+ that evolves to the final [(Co{(μ-ET)cyclen}-(N-5′-TMP))(μ-OH)(Co{(μ-ET)cyclen}(O-5′-TMP))]2+ species. On standing for longer periods, the final fully substituted species isomerises with the formation of {(Co{(μ-ET)cyclen}(O-5′-TMP))2(μ-OH)} units, as evidenced by a new signal on the 31P NMR spectrum appearing at 17.4 ppm (Scheme 4, bottom right). Table 1 shows the relevant kinetic and activation parameters for the substitution processes studied.

Interestingly, the values for the entry of the first 5′-TMP ligand (N-bound) have a rather low value of ΔH‡ and extremely negative activation entropy. It is clear that, even in this inherently dissociatively activated substitution process (CoIII t2g6), an important outer-sphere degree of associative activation must be present, also evidenced by the values determined for ΔV‡. This is in good agreement with the presence of an {ONO} unit in the ligand plus some NH groups in the inert skeleton of the complex.33 For the entry of the second (O-bound) 5′-TMP, this effect seems to be minimised, and a large value of ΔH‡ is determined together with values of ΔS‡ and ΔV‡ close to zero.

As for the absence of pH dependence in the values of k1, previously reported data referring to proton ambiguity for these systems,61 as well as protonation of the outer-sphere complexes,65 can be held responsible for the facts.22 Nevertheless, taking into account the potential actuation of conjugatebase mechanisms, as well as the very narrow range of pH used in the study (6.2–7.0), the above assumptions are highly speculative (see Fig. 4).

5′-UMP. The effect of the substitution of uridine for thymidine on the corresponding nucleotides was also studied. Fig. S7† shows the trend observed on [5′-UMP] of the two derived values of kobs at pH = 6.5. As for 5′-TMP the nature of the species being formed after each one of the sequential steps was assessed by 31P and Presat 1H NMR experiments (Fig. S8†). After a period of 1 h at 40 °C and pH = 6.8 a signal appears at 12.4 ppm in the 31P NMR spectrum, indicating the monodentate O-5′-UMP coordination to the cobalt centre. The parallel resat 1H NMR experiment indicates the presence of two doublets (7.8 and 7.9 ppm), the more intense at 7.9 ppm is assigned to the mono-N-5′-UMP. The signal of the 31P NMR spectrum indicates that the proton signal at 7.8 ppm must then correspond to a mono-

N-mono-O species as already established for the 5′-TMP derivatives. The rate constants derived from the experiments are practically equivalent to that obtained for the 5′-TMP, indicating a similar nature of the reaction. Nevertheless the corresponding value for KOS is much lower than for the thymidine derivative, in line with the observed for the reaction with the parent nucleosides. Given the complex nature of the secondary reactions observed, no pH, temperature or pressure dependence has been pursued for this system.

Comparison within the cyclen, {(μ-ET)cyclen} and {(Me)2(μ-ET)cyclen} series of complexes

In Scheme 5 a comparison of the structures of the series of CoIII aqua complexes with cyclen derivatives is indicated, as well as the final thermodynamically equilibrated form existing in solution at pHs close to the physiological pH.9,22 Successive substitution on the NH groups of the cyclen ligand produces a significant decrease in the relevance of the dimerization processes under biologically significant conditions; which is related to the expected tuning on conjugatebase pathways dominant for the cyclen derivatives,29 relevant for the simple cross-bridged derivate, and irrelevant for the complexes of the fully alkylated derivative.22 These trends indicate a thermodynamic preference of the dimeric μ-OH species.9

A further very interesting tuning found for the series of studies, relates to differences in hydrogen bonding interactions due to the presence of NH groups in the ligand. While for the fully alkylated compound hydrogen bonding interactions with thymidine seems to be solely taking place via interactions with the hydroxo ligand on the monomeric CoIII centre, for the cross bridged ligand compound here reported, the involvement of the axial NH group increases by an order of magnitude the stability of such an interaction (Scheme 6, left). This is especially important considering that the extreme dissociative substitution occurring on conjugate-base pathways is not too relevant for this complex (see above), thus allowing for an unexpected association.

Precisely this outer-sphere association is selective, and the formation of N-bound thymidine for the 5′-TMP nucleotide can be observed despite the phosphate-bound derivative being thermodynamically preferred as shown in Scheme 4. Moreover, a possible outer-sphere pairing interaction can be also held responsible for the unobserved bis-N-bound thymidine derivative, as indicated in Scheme 6 (right).

CONCLUSIONS

The substitution reactivity of the [Co{(μ-ET)cyclen}(H2O)2]3+complex cation at pH close to neutrality is dominated by the formation of the dead-end bis-hydroxobridged [(Co{(μ-ET)-cyclen})2(μ-OH)2]4+ complexes at pH > 7.5, which parallels what has been observed for the parent cyclen derivative and that of the fully alkylated [(Co{(Me)2(μ-ET)cyclen})2(μ-OH)2]4+. At Ph values within the 6.0–7.0 range substitution reactivity occurs solely on the mono-hydroxobridged [(Co{(μ-ET)cyclen}-(H2O))2(μ-OH)]5+ species, as observed for the cyclen analogous system, but differing from the fully alkylated derivative where this species is only residual. It is clear that the presence of NH groups in the axial coordination positions of the complex (Scheme 1) dominates this reactivity, whereas that of the highly acidic NH in the equatorial positions of the [Co(cyclen)-(H2O)2]3+ complex is only responsible for the readiness and equilibrium position of the mono-hydroxobridged species formation reaction.

The kinetico-mechanistic studies conducted on the substitution of the aqua/hydroxo ligands of this dinuclear species with biologically significant ligands are indicative of an important role of outer-sphere complexation. The appearance of limiting kinetics is rather general, and with values of KOS that are in line with the intervention of both the leaving aqua ligands and the residual NH groups in the encapsulating {(μ-ET)-cyclen} ligand (Scheme 6). The formation of hydrogenbonded encounter complexes results in the preferential formation of O- or N-bonded nucleotides depending on the structure of the base moiety of the ligand. Furthermore, as observed for the reaction with mononuclear [Co{(Me)2(μ-ET) cyclen}(H2O)-(OH)]2+, the selective entry of the different donor bonded nucleotides can also be hampered by the hydrogenbonding interaction with the dangling moiety of the coordinated ligand. As expected, the processes occur at a faster rate than for the fully alkylated encapsulating ligand derivative, given the still available base-catalysing NH groups in {(μ-ET)cyclen}.

EXPERIMENTAL

Compounds and procedures

The cobalt [Co{(μ-ET)cyclen}(H2O)2](CF3SO3)3 complex has been prepared directly by crystallisation of the already described [Co{(μ-ET)cyclen}(CF3SO3)2](CF3SO3) in a minimum amount of slightly acidic (HCF3SO3) water.18 The complex was characterised by its elemental analyses (Calc., found %) for [Co{(μ-ET)cyclen}(H2O)2](CF3SO3)3·1.5H2O: C: 20.3, 20.0; N: 7.3, 7.2; H: 3.8, 3.7; S: 12.5, 12.6. 13C NMR (57.6, 62.8, 63.2 ppm) and UV-Vis spectra (λmax = 360 nm (110 M−1 cm−1); λmax = 490 nm (180 M−1 cm−1)). XRD quality crystals were also obtained; Fig. 1 shows the molecular drawing of the complex cation and Table 2 the corresponding crystal data and structure refinement. The nucleosides and nucleotides used were commercially available and were used as received.

MES and HEPES solutions were prepared to a 0.4 M concentration at I = 1.0 (NaClO4) by weighing the desired amounts of the commercially available reactants. Final pH was adjusted with suitable HClO4 or NaOH solutions.32 These stock solutions were used as the solvent for all the ligand solutions used in the study. As a standard procedure the pH of the samples at the desired temperature was monitored before and after randomly selected experiments; no significant differences were obtained in any case and the procedure was thus considered valid under the conditions used.

13C and 31P NMR spectroscopy were carried out on Bruker 400-Crio instrument in H2O adjusted at the desired pH, and with a D2O inset containing the corresponding reference, at the Unitat d'RMN from the Centres Científics i Tecnològics de la Universitat de Barcelona (CCiTUB). The spectra were referenced externally to NaTMPS (13C) and H3PO4 (31P). 1H NMR spectra from the same aqueous solutions were recorded using a water Presat experiment on the same instrument. UV-Vis spectra were recorded using either a Cary 50 or a HP8453 instrument equipped with thermostated multicell transports. For the reactions carried out at varying pressure the already described pillbox cell and pressurising systems66–69 were used connected to a J&M TIDAS instrument. pH measurements were conducted on a Crison instrument using either fast response or microsample glass combined electrodes. Time-resolved UV-Vis spectra were recorded with the same instruments and exported to the relevant software packages indicated below.

pKa determination was carried out by UV-Vis spectroscopy titration on 1 × 10−3 M solutions of the cobalt complex, taken to 0.01 M HClO4, by adding small aliquots of 0.1 M NaOH. Electronic spectra (Fig. S8†) were recorded by using a Helma 661.202-UV All Quartz Immersion Probe connected to a Cary 50 instrument with optical fibres. The pKa determination was carried out using the standard Specfit or ReactLab Equilibrium software.43,44

Kinetics

Solutions of the different ligands involved in the kinetic runs were prepared in the corresponding 0.4 M buffer solutions at I = 1.0 described above. The solutions of the metal complex were prepared at much higher concentrations (20–30 fold) in water; thus an effective acidic pH was achieved, which prevented its polymerisation processes. Small aliquots of this stock solution were added to achieve the final conditions of the runs ([CoIII] = (2–7) × 10−4 M, [ligand] = 0.01–0.1 M). For all the substitution processes pseudo-first order flooding conditions were used.

All the time-resolved experiments (by pH, and NMR or UV-Vis spectral monitoring) were conducted following three types of setups. (i) For non-buffered medium the desired aliquot of the stock CoIII complex solution was added to a solution at a chosen acidity; pH was immediately registered and further UV-Vis, NMR and pH changes were monitored. (ii) For experiments in buffered media the desired

aliquot of the stock CoIII complex solution was added to the chosen 0.4 M buffer solution; pH was registered and further UV-Vis, NMR and pH changes were monitored. (iii) For experiments, requiring a preequilibration process, the desired aliquot of the stock CoIII complex solution was added to the chosen 0.4 M buffer solution without reactants; pH was registered and UV-Vis monitoring was carried out. When the spectral changes associated with the equilibration process were completed a solution of the desired ligand in the chosen 0.4 M buffer was added to the final desired concentration; pH was registered and further UV-Vis, NMR and/or pH changes were monitored.

All data were collected as full (300–750 nm) spectra and treated with the standard Specfit or ReactLab Kinetics software; 43,44 observed rate constants were obtained from the full changes of the spectra or alternatively at the wavelength where a maximum change was observed. The changes were fitted to the relevant A → B single exponential equation when first or pseudo-first order conditions applied; for consecutive reactions with the same characteristics, an A → B → C two exponential sequence was fitted. Table S1† shows all the values obtained for kobs as a function of the different compounds and variables studied.

X-ray diffraction analyses

A red prism-like specimen of C13H26CoF9N4O12S3, with approximate dimensions 0.299 × 0.127 × 0.107 mm, was used for the X-ray crystallographic analysis. The X-ray intensity data were collected on a D8 Venture system equipped with a multilayer monochromator and a Mo microfocus (λ = 0.71073 Å).

The frames were integrated with the Bruker SAINT software package using a narrow-frame algorithm. The integration of the data using a monoclinic unit cell yielded a total of 32 892 reflections to a maximum θ angle of 26.40° (0.80 Å resolution), of which 5568 were independent (average redundancy 5.907, completeness = 99.6%, Rint = 4.65%, Rsig = 3.17%) and 5408 (97.13%) were greater than 2σ(F2). The final cell constants a = 9.0812(4) Å, b = 22.5814(13) Å, c = 13.3340(7) Å, β = 95.368(2)°, volume = 2722.4(2) Å3 are based upon the refinement of the XYZ-centroids of reflections above 20σ(I). Data were corrected for absorption effects using the multi-scan method (SADABS). The calculated minimum and maximum transmission coefficients (based on crystal size) are 0.6885 and 0.7454.

The structure was solved using the Bruker SHELXTL software package, and refined using SHELXL,70 using the space group P121/n1, with Z = 4 for the formula unit, C13H26CoF9N4O12S3. The final anisotropic full-matrix leastsquares refinement on F2 with 382 variables converged at R1 = 7.27%, for the observed data and wR2 = 16.31% for all data. The goodness-of-fit was 1.068. The largest peak in the final difference electron density synthesis was 1.812 e Å−3 and the largest hole was −1.239 e Å−3 with an RMS deviation of 0.116 e Å−3. On the basis of the final model, the calculated density was 1.851 g cm−3 and F(000), 1544 e−.

ACKNOWLEDGEMENTS

Financial support from the Spanish Ministerio de Economía y Competitividad (project CTQ2012-37821-C02-01) is acknowledged. MV also acknowledges a FI-DGR grant from the Generalitat de Catalunya.

REFERENCES

1 K. Gloe, in Macrocyclic chemistry: current trends and future perspectives, Springer, Dordrecht, 2005.

2 J. A. Cowan, in Inorganic Biochemistry. An Introduction, Wiley-VCH, 2nd edn, 1997.

3 M. Albrecht, G. Rodríguez, J. Schoenmaker and G. van Koten, Org. Lett., 2000, 2, 3461–3464.

4 S. V. Wegner and J. P. Spatz, Angew. Chem., Int. Ed., 2013, 52, 7593–7596.

5 E. Wexselblatt, E. Yavin and D. Gibson, Angew. Chem., Int. Ed., 2013, 52, 6059–6062.

6 Z. D. Bugarcic, J. Bogojeski, B. Petrovic, S. Hochreuther and R. van Eldik, Dalton Trans., 2012, 41, 12329–12345.

7 N. Busto, M. Martínez-Alonso, J. M. Leal, A. M. Rodríguez, F. Domínguez, M. I. Acuña, G. Espino and B. García, Organometallics, 2014, 34, 319–327.

8 V. Pierroz, T. Joshi, A. Leonidova, C. Mari, J. Schur, I. Ott, L. Spiccia, S. Ferrari and G. Gasser, J. Am. Chem. Soc., 2012, 134, 20376–20387.

9 M. G. Basallote, M. Martínez and M. Vázquez, Dalton Trans., 2014, 43, 11048–11058.

10 C. M. Clavel, E. Paunescu, P. Nowak-Sliwinska and P. J. Dyson, Chem. Sci., 2014, 5, 1097–1101.

11 P. C. A. Bruijnincx and P. J. Sadler, Curr. Opin. Chem. Biol., 2008, 12, 197–206.

12 A. W. Han and P. J. Dyson, Eur. J. Inorg. Chem., 2006, 4003–4018.

13 H. K. Liu, S. J. Berners-Price, F. Wang, J. A. Parkinson, J. Xu, J. Bella and P. J. Sadler, Angew. Chem., Int. Ed., 2006, 45, 8153–8156.

14 C. Scolaro, A. Bergamo, L. Brescacin, R. Delfino, M. Cocchietto, G. Laurenczy, T. J. Geldbach, G. Sava and P. J. Dyson, J. Med. Chem., 2005, 48, 4161–4171.

15 A. Habtemariam, M. Melchart, R. Fernández, S. Parsons, I. D. H. Oswald, A. Parkin, F. P. A. Fabbiani, J. E. Davidson, A. Dawson, R. E. Aird, D. I. Jodrell and P. J. Sadler, J. Med. Chem., 2006, 49, 6858–6868.

16 Y. K. Yan, M. Melchart, A. Habtemariam and P. J. Sadler, Chem. Commun., 2005, 4764–4776.

17 A. Bergamo and G. Sava, Dalton Trans., 2011, 40, 7817–7823.

18 J. Y. C. Chang, G. L. Lu, R. J. Stevenson, P. J. Brothers, G. R. Clark, K. J. Botting, D. M. Ferry, M. Tercel, W. R. Wilson, W. A. Denny and D. C. Ware, Inorg. Chem., 2013, 52, 7688–7698.

19 T. W. Failes, C. Cullinane, C. I. Diakos, N. Yamamoto, J. G. Lyons and T. W. Hamblet, Chem. – Eur. J., 2007, 13, 2974–2982.

20 I. Ott, K. Schmidt, B. Kircher, P. Schumacher, T. Wiglenda and R. Gust, J. Med. Chem., 2005, 48, 622–629.

21 K. Gómez, G. González, M. Martínez, C. Mendoza and B. Sienra, Polyhedron, 2006, 25, 3509–3518.

22 M. Martínez and M. Vázquez, Inorg. Chem., 2015, 54, 4972–4980.

23 T. J. Hubin, P. N. A. Amoyaw, K. D. Roewe, N. C. Simpson, R. D. Maples, T. N. Carder Freeman, A. N. Cain, J. G. Le, S. J. Archibald, S. I. Khan, B. L. Tekwani and M. O. F. Khan, Bioorg. Med. Chem., 2014, 22, 3239–3244.

24 T. J. Hubin, N. W. Alcock, M. D. Morton and D. H. Busch, Inorg. Chim. Acta, 2003, 348, 33–40.

25 W. Niu, E. Wong, G. Weisman, Y. Peng, C. Anderson, L. Zakharov, J. Golen and A. Rheingold, Eur. J. Inorg. Chem., 2004, 3310–3315.

26 B. F. E. Curchod and F. P. Rotzinger, Inorg. Chem., 2011, 50, 8728–8740.

27 M. L. Tobe, in Advances in Inorganic and Bioinorganic Mechanisms, Academic Press, London, 1983, ch. 2, pp. 1–94.

28 M. L. Tobe and J. Burgess, in Inorganic Reaction Mechanisms, Longman, 1999.

29 N. J. Curtis, P. Hendry and G. A. Lawrance, J. Chem. Soc., Dalton Trans., 1988, 47–51.

30 W. G. Jackson, Aust. J. Chem., 2009, 62, 1308–1317.

31 M. M. DeMaine and J. B. Hunt, Inorg. Chem., 1971, 10, 2106–2113.

32 N. E. Good, G. D. Winget, W. Winter, T. N. Connolly, S. Izawa and R. M. M. Singh, Biochemistry, 1966, 5, 467–477.

33 S. Aoki and E. Kimura, J. Am. Chem. Soc., 2000, 122, 4542–4548.

34 J. Y. C. Chang, R. J. Stevenson, G. L. Lu, P. J. Brothers, G. R. Clark, W. A. Denny and D. C. Ware, Dalton Trans., 2010, 39, 11535–11550.

35 R. G. Wilkins, in Kinetics and Mechanisms of Reactions of Transition Metal Complexes, VCH, 1991.

36 M. L. Tobe, in Advances in Inorganic and Bioinorganic Mechanisms, Academic Press, London, 1983, ch. 2, pp. 1–94.

37 T. Zhang, X. Zhu and R. Prabhakar, Organometallics, 2014, 33, 1925–1935.

38 J. Kozelka, F. Legendre, F. Reeder and J. C. Chottard, Coord. Chem. Rev., 1999, 190–192, 61–82.

39 N. de Barrios, G. González, A. Grandas, M. Martínez and V. Moreno, Inorg. React. Mech., 1999, 1, 205–218.

40 H. Hohmann and R. van Eldik, Inorg. Chim. Acta, 1990, 174, 87–92.

41 H. Hohmann, B. Hellquist and R. van Eldik, Inorg. Chim. Acta, 1991, 188, 25–32.

42 F. von Seel and G. Bohnstedt, Z. Anorg. Allg. Chem., 1977, 435, 257–267.

43 R. A. Binstead, A. D. Zuberbuhler and B. Jung, SPECFIT32 [3.0.34], Spectrum Software Associates, Marlborough, MA, USA, 2005.

44 M. Maeder and P. King, ReactLab, Jplus Consulting Pty Ltd, East Fremantle, WA, Australia, 2009.

45 J. M. Coronas, R. Vicente and M. Ferrer, Inorg. Chim. Acta, 1981, 49, 259.

46 J. Vinaixa and M. Ferrer, J. Chem. Educ., 1983, 60, 155–166.

47 M. Martínez and M. Ferrer, Transition Met. Chem., 1984, 9, 395–397.

48 C. Thibaudeau, J. Plavec and J. Chattopadhyaya, J. Org. Chem., 1996, 61, 266–286.

49 M. E. Sosa and M. L. Tobe, J. Chem. Soc., Dalton Trans., 1985, 475–477.

50 J. H. Espenson, in Chemical Kinetics and Reaction Mechanisms, McGraw-Hill, 1981.

51 A. G. Lappin, in Redox Mechanisms in Inorganic Chemistry, Ellis Horwood, 1994.

52 G. González, B. Moullet, M. Martínez and A. E. Merbach, Inorg. Chem., 1994, 33, 2330–2333.

53 G. González, M. Martínez and E. Rodríguez, J. Chem. Soc., Dalton Trans., 1995, 891–892.

54 F. Benzo, P. V. Bernhardt, G. González, M. Martínez and B. Sienra, J. Chem. Soc., Dalton Trans., 1999, 3973–3979.

55 A. Macchioni, Eur. J. Inorg. Chem., 2003, 195–205.

56 A. Macchioni, Chem. Rev., 2005, 105, 2039–2074.

57 M. Martínez, M. A. Pitarque and R. van Eldik, J. Chem. Soc., Dalton Trans., 1996, 2665–2671.

58 P. V. Bernhardt, F. Bozoglián, B. P. Macpherson, M. Martínez, A. E. Merbach, G. González and B. Sienra, Inorg. Chem., 2004, 43, 7187–7195.

59 P. V. Bernhardt, F. Bozoglián, B. P. Macpherson, M. Martínez, G. González and B. Sienra, Eur. J. Inorg. Chem., 2003, 2512–2518.

60 G. González, M. Martínez and E. Rodríguez, Eur. J. Inorg. Chem., 2000, 1333–1338.

61 R. B. Jordan, in Reaction mechanisms of inorganic and organometallic systems, Oxford University Press, 2007.

62 I. Luyten, K. W. Pankiewicz, K. A. Watanabe and J. Chattopadhyaya, J. Org. Chem., 1998, 63, 1033–1040.

63 P. A. Levene and H. S. Simms, J. Biol. Chem., 1925, 65, 519–534.

64 M. L. Souza, E. E. Castellano, J. Telser and D. W. Franco, Inorg. Chem., 2015, 54, 2067–2080.

65 M. Ferrer, M. Martínez and M. A. Pitarque, J. Chem. Soc., Dalton Trans., 1990, 1629–1633.

66 R. van Eldik, in Inorganic High Pressure Chemistry, ed. R. van Eldik, Elsevier, 1986, pp. 1–68.

67 J. Garcia-Amorós, M. Martínez, H. Finkelman and D. Velasco, J. Phys. Chem. B, 2010, 114, 1287–1293.

68 B. P. Macpherson, B. M. Alzoubi, P. V. Bernhardt, M. Martínez, P. Tregloan and R. van Eldik, Dalton Trans., 2005, 1459–1467.

69 I. Favier, M. Gómez, J. Granell, M. Martínez, M. Font-Bardía and X. Solans, Dalton Trans., 2005, 123–132.

70 G. M. Sheldrick, Acta Crystallogr., Sect. A: Fundam. Crystallogr., 2008, 64, 112–122.

.

Legends to figures

Figure 1 Drawing of the [Co{(μ-ET)cyclen}(H2O)2]3+ cation prepared in this work (hydrogen atoms have been omitted for clarity). Relevant distances (Å) and angles (°) are: Co(1)–N(1) = 1.95; Co(1)–N(2) = 1.90; Co(1)–N(3) = 1.89; Co(1)–N(4) = 1.96; Co(1)–O(1) = 2.06; Co(1)–O(2) = 1.90; N(1)–Co(1)–N(4) = 169.0; N(2)–Co(1)–N(3) = 90.0; O(1)–Co(1)–O(2) = 85.4.

Figure 2. (a) Changes in the electronic spectrum of a solution of [Co{(μ-ET)cyclen}(H2O)2]3+ complex (5 × 10−4 M) in buffered aqueous solution at Ph = 7.0 of inorganic phosphate 0.01 M (40 °C, HEPES, I = 1.0 (NaClO4)). (b) Plot of the values of the dependence of kobs on [phosphate] at different pHs at 40 °C (▲, pH = 6.0; ■, pH = 6.5; ●, pH = 7.0; 0.4 M MES/HEPES, I = 1.0 (NaClO4)).

Figure 3 a) Changes with time of the electronic spectrum of a 5 × 10−4 M solution of complex [Co{(μ-ET)cyclen}(H2O)2]3+ with thymidine 0.04 M at pH = 7.0 (HEPES 0.4 M, 40 °C, I = 1.0 (NaClO4)). (b) Plot of the values of the dependence of kobs on [thymidine] at different pHs at 40 °C (▲, pH = 6.0; ■, pH = 6.5; ●, pH = 7.0; 0.4 M HEPES, I = 1.0 (NaClO4)).

Fig. 4 Plot of the values of the dependence of kobs on [5'-TMP−/5'-TMP2−] at different pHs at 40 °C (▲, pH = 6.2; ■, pH = 6.5; ◆, pH = 6.8; ●, pH = 7.0; 0.4 M MES/HEPES, I = 1.0 (NaClO4)).

611 **SCHEME 1**

612

613

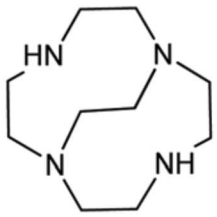

{(μ-ET)cyclen}

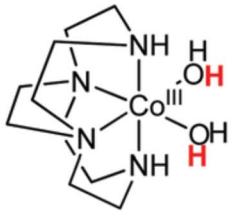

$[Co\{(\mu\text{-ET})cyclen\}(H_2O)_2]^{3+}$

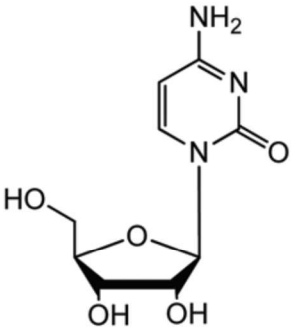

cytidine

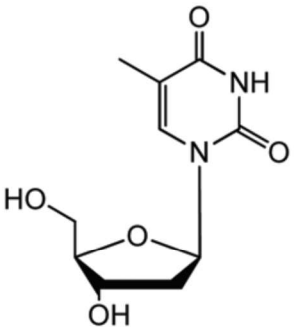

thymidine

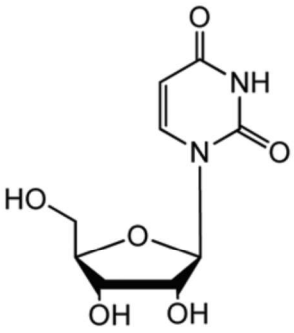

uridine

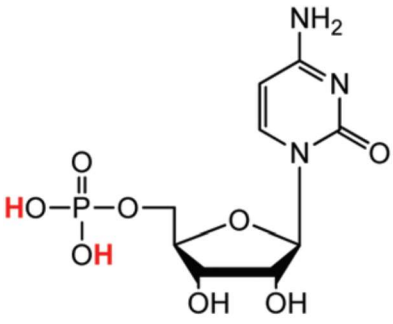

5'-CMP

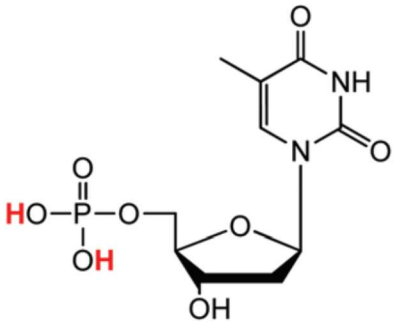

5'-TMP

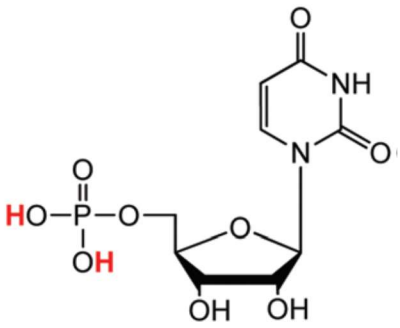

5'-UMP

614

615

FIGURE 1

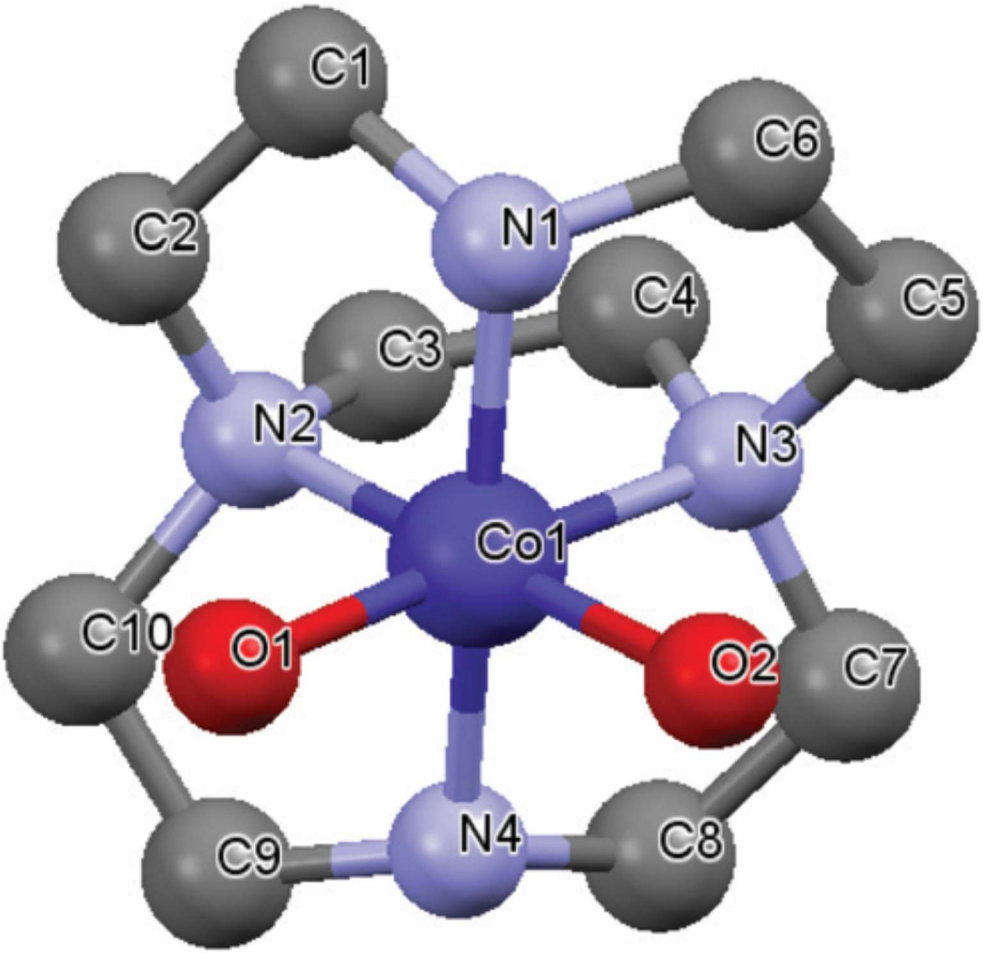

SCHEME 2

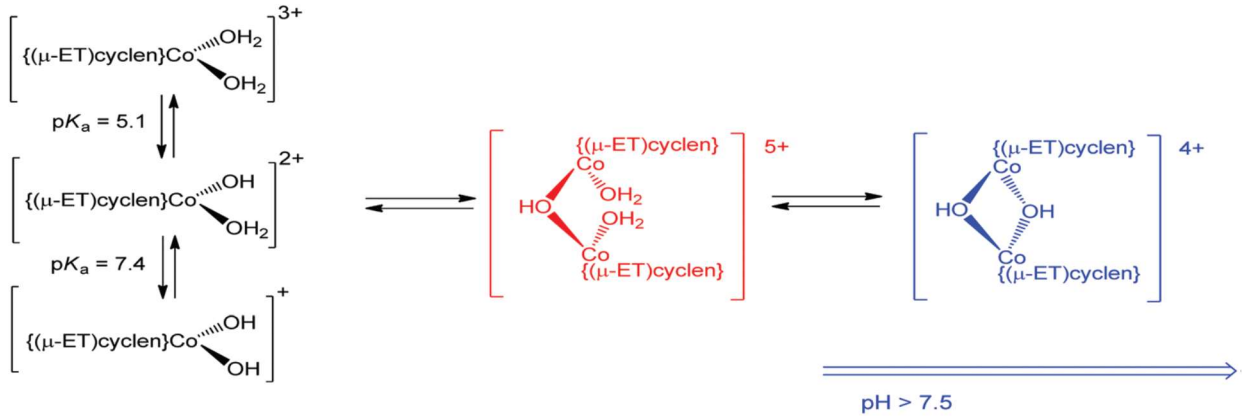
{(μ-ET)cyclen}Co
OH2
OH2
3+
pKa = 5.1
{(μ-ET)cyclen}Co
OH
OH2
2+
pKa = 7.4
{(μ-ET)cyclen}Co
OH
OH
+
{(μ-ET)cyclen}
Co
HO
OH2
OH2
Co
{(μ-ET)cyclen}
5+
{(μ-ET)cyclen}
Co
HO
OH
Co
{(μ-ET)cyclen}
4+
pH > 7.5

FIGURE 2

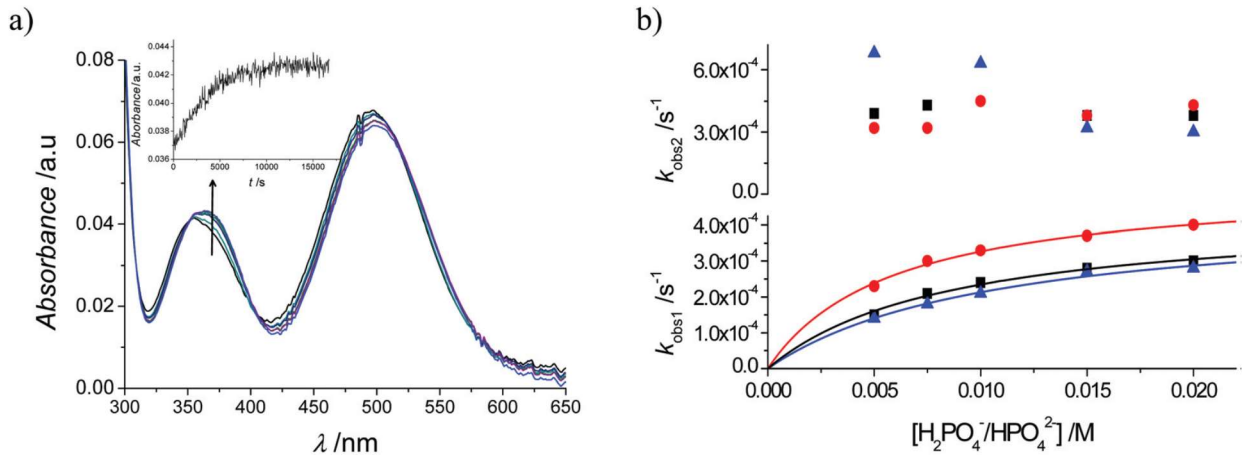
a)
Absorbance /a.u
λ /nm
Aborbance/a.u.
t /s
b)
k_{obs2} /s^{-1}
k_{obs1} /s^{-1}
[$H_2PO_4^-$/HPO_4^{2-}] /M

633 **SCHEME 3**

634

635

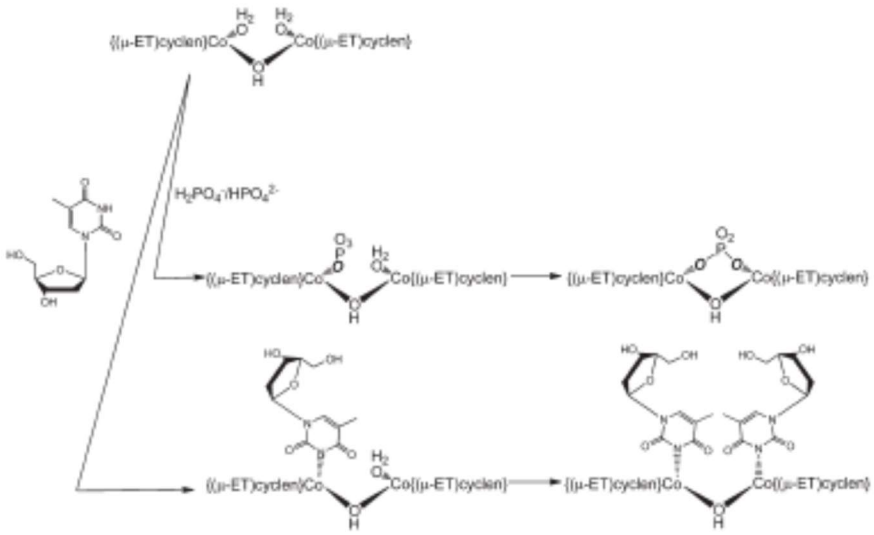

636

637

638

FIGURE 3

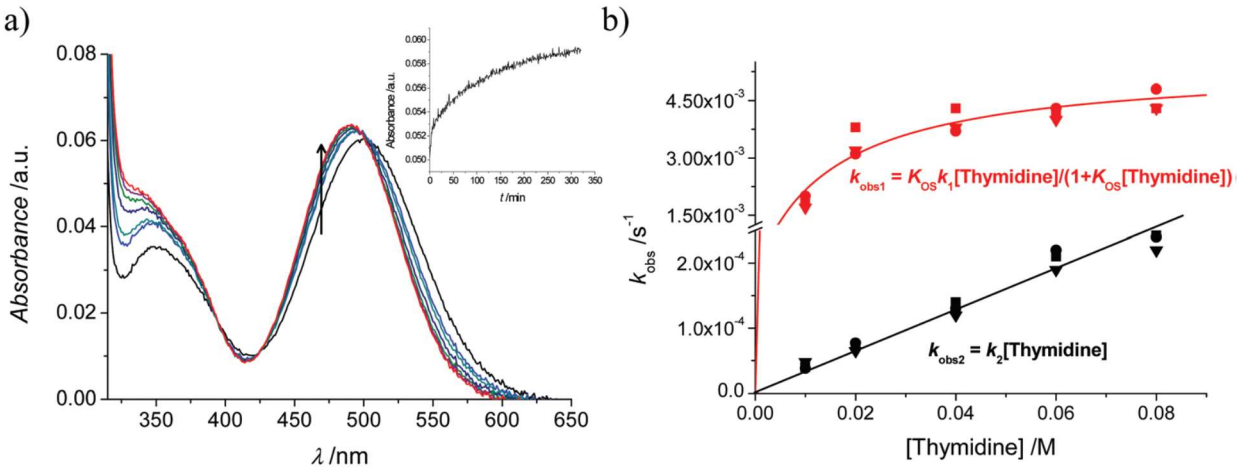
a)
Absorbance /a.u.
λ /nm
Absorbance /a.u.
t /min
b)
k_{obs} /s^{-1}
$k_{obs1} = K_{OS}k_1$[Thymidine]/(1+K_{OS}[Thymidine])
$k_{obs2} = k_2$[Thymidine]
[Thymidine] /M

644 **SCHEME4**

645

646

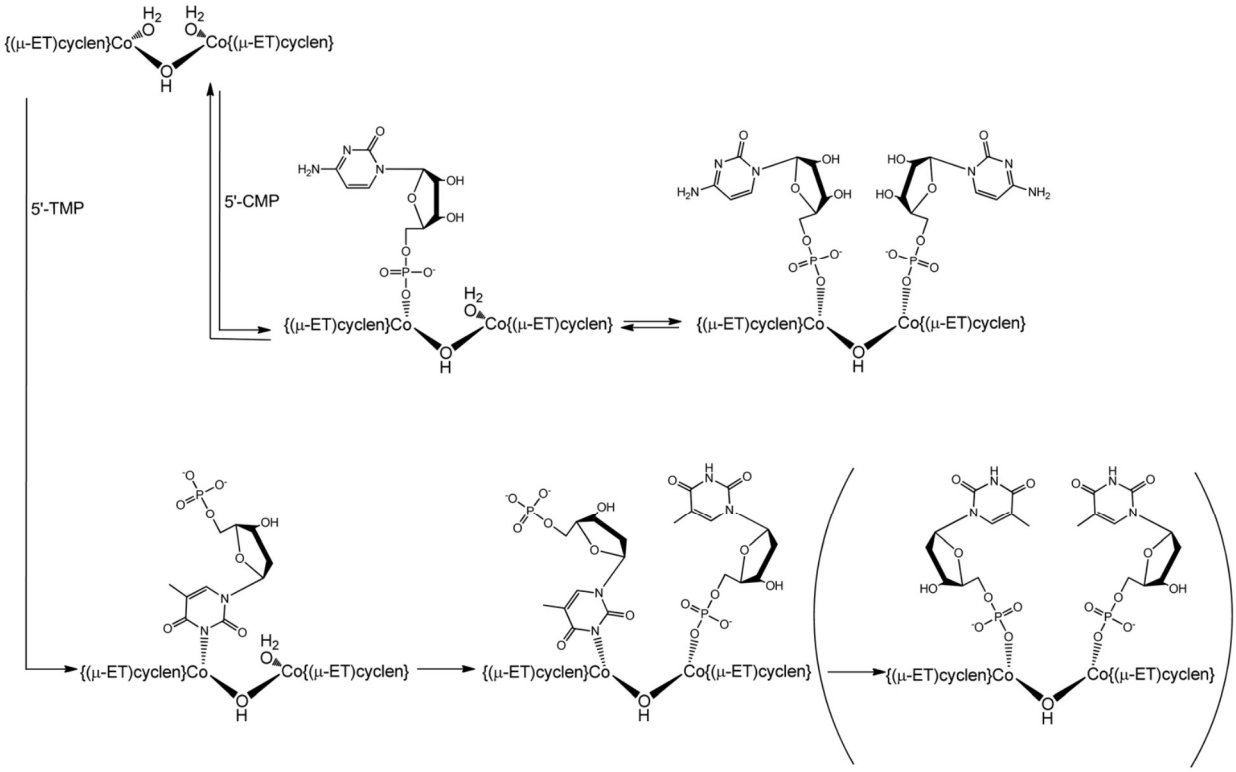

647

648

FIGURE 4

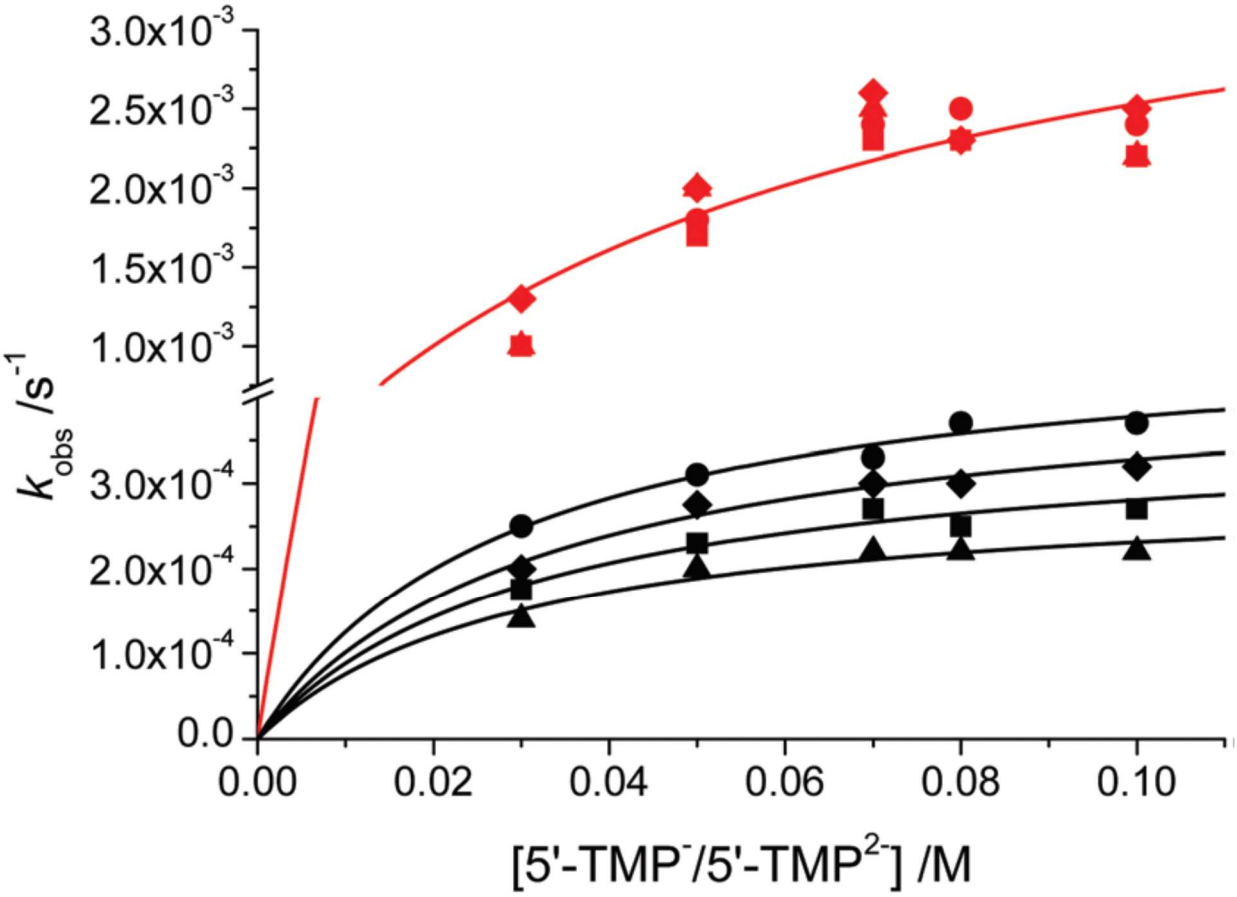
3.0x10-3
2.5x10-3
2.0x10-3
1.5x10-3
1.0x10-3
3.0x10-4
2.0x10-4
1.0x10-4
0.0
kobs /s-1
0.00
0.02
0.04
0.06
0.08
0.10
[5'-TMP-/5'-TMP2-] /M

SCHEME 5

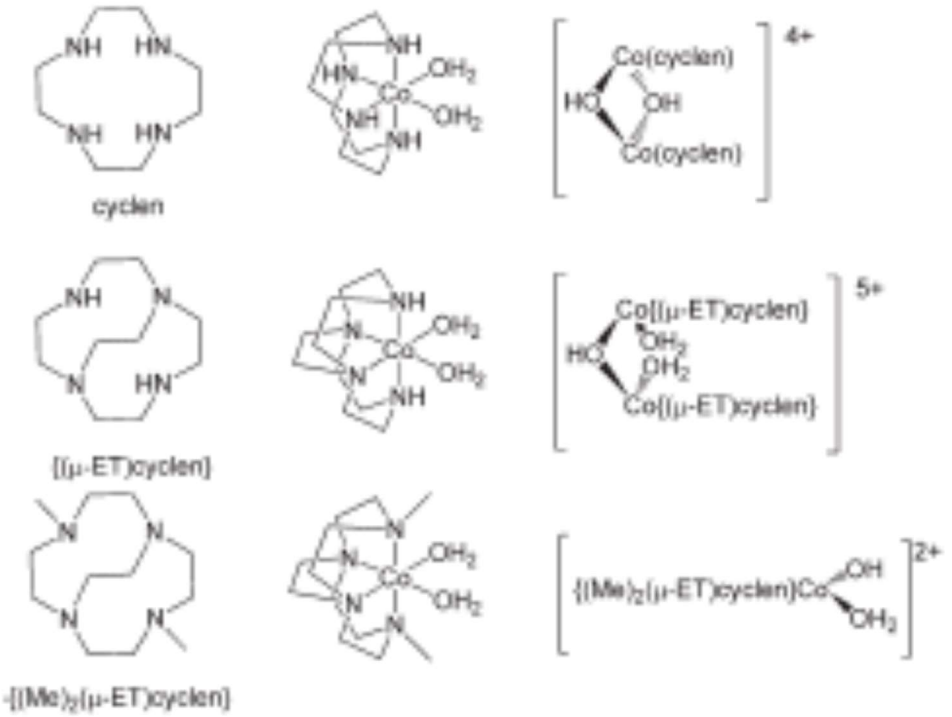
cyclen
[(μ-ET)cyclen]
{(Me)2(μ-ET)cyclen}
Co(cyclen)
Co[(μ-ET)cyclen]
{(Me)2(μ-ET)cyclen}Co
4+
5+
2+

SCHEME 6

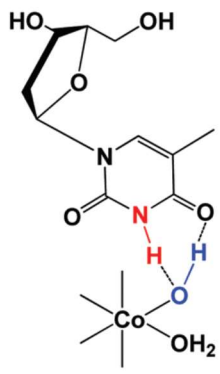

K_{OS} *ca.* 20

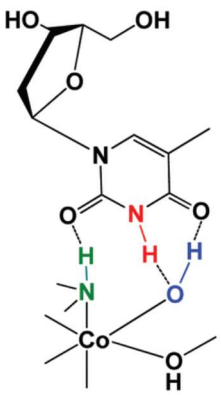

K_{OS} *ca.* 240

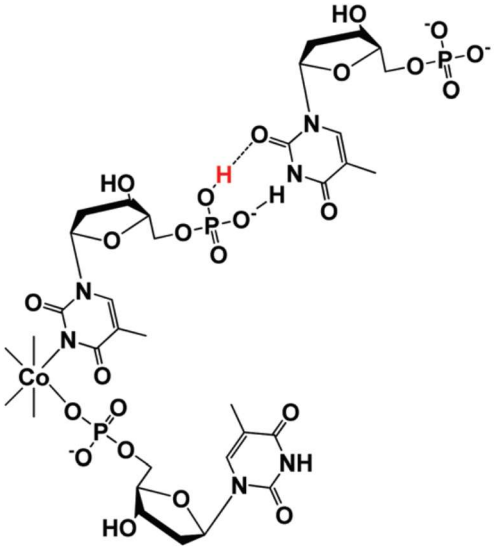

672

673 **Table 1.** Summary of the kinetic, thermal and pressure activation parameters for the reaction of [Co{(μ-

674 ET)cyclen}(H2O)2]3+ with phosphate, cytidine, thymidine, 5'-CMP and 5'-TMP at different pHs (0.4

675 M MES/HEPES, I = 1.0 NaClO4)

676

677

Entering ligand	pH	$^{a,b,c}k/M^{-1}\ s^{-1}$	$\Delta H^{\ddagger}$/kJ mol^{-1}	$\Delta S^{\ddagger}$/J K^{-1} mol^{-1}	$\Delta V^{\ddagger}$/cm^3 mol^{-1}
$H_2PO_4^-/HPO_4^{2-}$	6.0	$k_1 = 4.4 \times 10^{-4\,a}$ $k_2 = 4.8 \times 10^{-4\,b}$		Not determined	
	6.5	$k_1 = 4.4 \times 10^{-4\,a}$ $k_2 = 4.0 \times 10^{-4\,b}$			
	7.0	$k_1 = 5.2 \times 10^{-4\,a}$ $k_2 = 3.8 \times 10^{-4\,b}$			
Cytidine	6.0	$k_1 = 12 \times 10^{-3}$ $k_{-1} = 2.8 \times 10^{-4\,c}$ $k_2 = 1.7 \times 10^{-3}$ $k_{-2} = 2.7 \times 10^{-5\,c}$		Not determined	
	6.5	$k_1 = 13 \times 10^{-3}$ $k_{-1} = 4.4 \times 10^{-4\,c}$ $k_2 = 2.6 \times 10^{-3}$ $k_{-2} = 3.0 \times 10^{-5\,c}$	95 ± 1 112 ± 1 100 ± 5 115 ± 9	19 ± 4 50 ± 4 20 ± 16 41 ± 30	Not determined
	7.0	$k_1 = 17 \times 10^{-3}$ $k_{-1} = 2.0 \times 10^{-3}$ $k_2 = 2.7 \times 10^{-3}$ $k_{-2} = 6.0 \times 10^{-5\,c}$		Not determined	
Thymidine	6.0, 6.5, 7.0	$k_1 = 4.5 \times 10^{-3\,d}$ $k_2 = 3.2 \times 10^{-3}$	95 ± 4 90 ± 7	11 ± 14 −8 ± 22	−8 ± 1[e] 4 ± 1[e]
$5'$-CMP$^-$/$5'$-CMP^{2-}	6.0	$k_1 = 2.1 \times 10^{-3}$ $k_{-1} = 2.1 \times 10^{-4\,c}$ $k_2 = 9.9 \times 10^{-4}$ $k_{-2} = 7.9 \times 10^{-5\,c}$		Not determined	
	6.5	$k_1 = 7.7 \times 10^{-3}$ $k_{-1} = 4.8 \times 10^{-4\,c}$ $k_2 = 1.1 \times 10^{-3}$ $k_{-2} = 1.8 \times 10^{-4\,c}$	115 ± 4 79 ± 5 71 ± 6 129 ± 9	78 ± 14 −58 ± 16 −78 ± 20 93 ± 30	Not determined
	7.0	$k_1 = 9.3 \times 10^{-3}$ $k_{-1} = 9.2 \times 10^{-4\,c}$ $k_2 = 1.6 \times 10^{-3}$ $k_{-2} = 2.4 \times 10^{-4\,c}$		Not determined	
$5'$-TMP$^-$/$5'$-TMP^{2-}	6.2	$k_1 = 4.1 \times 10^{-3\,f}$ $k_2 = 3.0 \times 10^{-4\,g}$			
	6.5	$k_1 = 4.1 \times 10^{-3\,f}$ $k_2 = 3.5 \times 10^{-4\,g}$	43 ± 3[h] 105 ± 5[h]	−160 ± 8[h] 20 ± 14[h]	−15 ± 2[i] 0 ± 0.8[i]
	6.8	$k_1 = 4.1 \times 10^{-3\,f}$ $k_2 = 4.2 \times 10^{-4\,g}$		Not determined	
	7.0	$k_1 = 4.1 \times 10^{-3\,f}$ $k_2 = 4.7 \times 10^{-4\,g}$			

[a] Limiting value, in s^{-1}; average value for all systems of $K_{OS} = 120\ M^{-1}$. [b] Concentration independent bridge formation path, see the text. [c] Reverse rate constants in s^{-1}. [d] Limiting value, in s^{-1}; $K_{OS} = 240\ M^{-1}$. [e] Determined at pH = 6.5 and 30 °C using $k_2 \times K_{OS}$[Thymidine]=0.08 M, according to Fig. 3b. [f] Limiting pH independent value, in s^{-1}; $K_{OS} = 20\ M^{-1}$. [g] Limiting value, in s^{-1}; average value for all systems of $K_{OS} = 35\ M^{-1}$. [h] At 0.1 M 5'-TMP according to its limiting kinetics. [i] Determined at pH = 6.5 and 27 °C using $k \times K_{OS}$[5'-TMP]=0.1 M, according to Fig. 4.

678

679

680

681

682 **Table 2** Crystal data and structure refinement for complex [Co{(μ-ET)-cyclen}(H2O)2](CF3SO3)3

683

Empirical formula	$C_{13}H_{28}CoF_9N_4O_{13}S_3$
Formula weight	758.50
Temperature	100(2) K
Wavelength	0.71073 Å
Crystal system	Monoclinic
Space group	$P2_1/n$
Unit cell dimensions	$a = 9.0812(4)$; $b = 22.5814(13)$; $c = 13.3340(7)$ Å $\alpha = 90$; $\beta = 95.368(2)$; $\gamma = 90°$
Volume	2722.4(2) Å^3
Z	4
Density (calculated)	1.851 Mg m^{-3}
Absorption coefficient	0.985 mm^{-1}
$F(000)$	1544
Crystal size	0.299 × 0.127 × 0.107 mm^3
θ range for data collection	2.368 to 26.396°
Index ranges	$-11 \le h \le 10$, $-28 \le k \le 28$, $-16 \le l \le 16$
Reflections collected	32 892
Independent reflections	5568 [R(int) = 0.0465]
Completeness to θ = 25.242°	99.7%
Absorption correction	Semi-empirical from equivalents
Max. and min. transmission	0.7454 and 0.6885
Refinement method	Full-matrix least-squares on F^2
Data/restraints/parameters	5568/83/382
Goodness-of-fit on F^2	1.068
Final R indices [$I > 2\sigma(I)$]	$R_1 = 0.0727$, w$R_2 = 0.1616$
R indices (all data)	$R_1 = 0.0747$, w$R_2 = 0.1631$
Extinction coefficient	n/a
Largest diff. peak and hole	1.812 and −1.239 e Å^{-3}
CCDC code	1400867

684

685

686